Resonant enhancement of damping within the free layer of a microscale magnetic tunnel valve

P. S. Keatley, V. V. Kruglyak, A. Neudert, R. J. Hicken, V. D. Poimanov, J. R. Childress, and J. A. Katine

---

Articles you may be interested in

Micromagnetic study of current-pulse-induced magnetization switching in magnetic tunnel junctions with antiferromagnetically and ferromagnetically coupled synthetic free layers
Appl. Phys. Lett. 99, 222505 (2011); 10.1063/1.3664225

Ferromagnetic resonance and damping properties of CoFeB thin films as free layers in MgO-based magnetic tunnel junctions
J. Appl. Phys. 110, 033910 (2011); 10.1063/1.3615961

Ultrafast magnetization dynamics in magnetic tunneling junctions
Appl. Phys. Lett. 98, 263506 (2011); 10.1063/1.3605557

Characterization of the magnetization vortex state in magnetic tunnel junctions patterned into nanometer-scale arrays
J. Appl. Phys. 99, 014307 (2006); 10.1063/1.2161418

Relation between exchange coupling and enhanced coercivity in the free layer of a patterned magnetic tunnel junction
J. Appl. Phys. 96, 7399 (2004); 10.1063/1.1811776

Resonant enhancement of damping within the free layer of a microscale magnetic tunnel valve

P. S. Keatley,[1,a] V. V. Kruglyak,[1] A. Neudert,[1,2] R. J. Hicken,[1] V. D. Poimanov,[3] J. R. Childress,[4] and J. A. Katine[4]

[1]School of Physics and Astronomy, University of Exeter, Stocker Road, Exeter EX4 4QL, United Kingdom
[2]Fraunhofer Institute for Photonic Microsystems IPMS, Maria-Reiche-Str. 2, 01109 Dresden, Germany
[3]Faculty of Physics and Technology, Donetsk National University, 24 Universitetskaya Street, Donetsk 83001, Ukraine
[4]HGST, San Jose Research Center, 3403 Yerba Buena Road, San Jose, California 95135, USA

Picosecond magnetization dynamics in the free and pinned layers of a microscale magnetic tunnel valve have been studied using time-resolved scanning Kerr microscopy. A comparison of the observed dynamics with those of individual free and pinned layers allowed the effect of interlayer coupling to be identified. A weak interlayer coupling in the tunnel valve continuous film reference sample was detected in bulk magnetometry measurements, while focused Kerr magnetometry showed that the coupling was well maintained in the patterned structure. In the tunnel valve, the free layer precession was observed to have reduced amplitude and an enhanced relaxation. During magnetization reversal in the pinned layer, its frequency approached that of the low frequency mode associated with the free layer. At the pinned layer switching field, the linewidth of the free layer became similar to that of the pinned layer. The similarity in their frequencies promotes the formation of precessional modes that exhibit strong collective properties such as frequency shifting and enhanced linewidth, while inhomogeneous magnetization of the pinned layer during reversal may also play a role in these observations. The collective character of precessional dynamics associated with mixing of the free and pinned layer magnetization dynamics must be accounted for even in tunnel valves with a small interlayer coupling. © 2015 AIP Publishing LLC.
[http://dx.doi.org/10.1063/1.4907701]

Picosecond magnetization dynamics in magnetic multilayer structures underpin the operation of spin torque oscillators,[1] magnetic random access memory elements,[2] and hard disk read head sensors.[3] At gigahertz (GHz) frequencies, magnetization precession must be carefully controlled to achieve signal-to-noise levels necessary for device operation.[3] Interaction or coupling between constituent magnetic layers can lead to a dynamic response that behaves differently to that of the isolated layers.[4] In this work, the dynamic response of the free layer (FL) and pinned layer (PL) within a magnetic tunnel valve (TV) has been explored using time-resolved scanning Kerr microscopy. Comparison with measurements performed on isolated FL and PL reference samples allowed the effect of interlayer coupling to be identified.

A continuous film TV stack and corresponding FL and PL reference stacks were deposited onto 1.2 mm thick thermally oxidised Si/SiO$_2$ substrates by DC sputtering, Table I. Electron-beam lithography and ion-beam milling were used to fabricate 6 μm discs of each stack composition. A PtMn antiferromagnetic layer (AFM) was used to exchange bias the PL. The direction of the exchange bias field was set parallel to the uniaxial anisotropy easy axis of the FL by annealing the films in an in-plane magnetic field of 10 kOe at a temperature of 250 °C for 8 h. The tunnel barrier was formed from a Al(7) layer oxidized

in O$_2$ at 500 mTorr for 15 min. The junction resistance and tunnel-magnetoresistance of devices with similar composition was $\sim$36 $\Omega\mu$m^2 and $\sim$24%, respectively.[5] Vibrating sample magnetometry and inductive hysteresis loop measurements were used to characterise the magnetic parameters of continuous film reference samples deposited on 1 in. diameter, 0.5 mm thick glass coupons, Table II. Measurements on a range of FL thicknesses revealed that an estimated $\sim$12.1 Å of Ni$_{88}$Fe$_{12}$ was lost to interdiffusion with the Ta cap.

After patterning the 6 μm discs, a coplanar stripline (CPS) structure was then fabricated from a sputtered Ta/Au ($\sim$1000 Å) film. Photolithography was used to form a CPS consisting of two tracks that each had a width of $\sim$400 μm, and an edge-to-edge separation of 30 μm. The CPS was aligned so that the discs were positioned at the center of the 30 μm gap between the tracks. The length of the CPS was parallel to the PL exchange bias field and the FL easy axis. An electronic impulse generator was used to deliver electrical pulses of $\sim$7 V amplitude and 70 ps duration to the CPS via microscale microwave probes. The probes had a ground-signal configuration so that charge moved in opposite directions in the tracks, generating an out-of-plane magnetic field at the center of the CPS structure.[6] The transmitted pulse was monitored using an oscilloscope to ensure that the excitation for each sample was similar.

The pulses were synchronous with a Ti:Sapphire pulsed laser operating at repetition rate of 80 MHz. Laser pulses

---

a)Author to whom correspondence should be addressed. Electronic mail: p.s.keatley@exeter.ac.uk.

TABLE I. The complete TV stack composition and the PL and FL reference (ref.) compositions (thickness in Å).

Stack	Seed	AFM	PL	Tunnel barrier	FL	Cap
TV	Ta (50)	PtMn (250)	$Co_{80}Fe_{20}$ (80)	Al(7) + oxidation	$Co_{80}Fe_{20}(10)/Ni_{88}Fe_{12}(27)$	Ta (100)
PL ref.	Ta (50)	PtMn (250)	$Co_{80}Fe_{20}$ (80)	Al(7) + oxidation		Ta (100)
FL ref.	Ta (50)			Al(10) + oxidation	$Co_{80}Fe_{20}(10)/Ni_{88}Fe_{12}(27)$	Ta (100)

were generated with $\sim$100 fs duration at a wavelength of 800 nm. The laser beam was expanded ($\times$10), linearly polarized, and then focussed to a diffraction limited spot of $\sim$600 nm diameter using a high numerical aperture (0.65, $\times$40) microscope objective lens. Magnetization dynamics were excited using the out-of-plane magnetic field at the center of the CPS. To avoid edge effects,[6–8] the out-of-plane component of the magnetization precession was detected at the center of the 6 μm discs in stroboscopic measurements of the polar Kerr effect. The reflected beam was collected using the same objective lens and the Kerr rotation was measured using a polarizing photodiode bridge detector. Amplitude modulation of the impulse generator output allowed the dynamic Kerr signal to be recovered using a lock-in amplifier at the modulation frequency ($\sim$1 kHz).

In focused Kerr magnetometry measurements, a quadrant photodiode bridge detector was instead used to acquire hysteresis loops for the component of in-plane magnetization parallel to the applied magnetic field.[9] In TR and static Kerr measurements, the field was applied within the plane of the magnetic layers and along the easy axis and exchange bias axis of the FL and PL, respectively. A saturating magnetic field of $\sim$2 kOe was first applied either parallel (negative field) or anti-parallel (positive field) to the exchange bias direction. The subsequent field sweep in each case will be described as the increasing (negative to positive) and decreasing (positive to negative) field sweep, respectively.

In Figure 1, Kerr hysteresis loops acquired from the 6 μm disc of each stack composition are shown. The TV loop is dominated by the large, exchange biased loop of the PL, as confirmed by the loop acquired from the PL reference disc. Despite being buried beneath the tunnel barrier, FL, and cap, the large loop height of the PL ($\sim$40 mdeg) is ascribed to the greater thickness and larger magnetization of the PL CoFe, Table I. The value of the exchange bias field was $\sim$270 Oe and is in reasonable agreement with that of the TV and PL reference films, Table II. In contrast, the loop height of the FL is small ($\sim$6 mdeg) due to the reduced magnetization and thickness. The FL of the TV loops exhibits a small +18 Oe shift, that is expected from the interlayer Néel (orange peel) coupling.[10] The observed shift was found to be

smaller than expected from the TV reference film, Table II. The discrepancy may be ascribed to the dipolar interaction at the edge of the patterned structure that favours antiparallel FL-PL alignment,[7,8] or localized regions of enhanced coupling in the reference films due to substrate roughness.

TR Kerr measurements were performed on the 6 μm disc of each stack composition for applied magnetic field values in the range $\pm$1.3 kOe. Previously in Ref. 11, a Kittel formula was used to fit the FL precession frequency as a function of the applied field. The uniaxial anisotropy constant was found to be 4140 ± 330 ergs/cm^3 for the patterned structure assuming a g-factor of 2.1 and the saturation magnetization extracted from the magnetometry measurements on the reference films, Table II. The discrepancy between the values for the FL reference film and the patterned structure corresponds to a difference in the anisotropy field of $\sim$2 Oe. The anisotropy constants are therefore in good agreement within experimental uncertainty.

In Figures 2(a) and 2(b), typical TR Kerr signals are shown for each stack composition after a saturating magnetic field was applied in the direction of the exchange bias field (negative applied field). In Figures 2(a) and 2(b), TR signals are shown for negative and positive field values of similar magnitude. The TR signals have been calibrated in degrees of Kerr rotation[12] to understand how the amplitude of the dynamic response, particularly for the FL, is modified due to the presence of the PL in the TV. Since the layers within the TV stack are thin, it is reasonable to assume that the precession amplitude of the FL and PL in the TV can be compared to the corresponding reference discs without the need to consider the multilayer scattering problem.

TR signals acquired from the TV and the FL reveal a significant reduction of the FL precession amplitude within

TABLE II. Saturation magnetization M, anisotropy constant K, exchange or biasing field H_{eb}, and coupling constant A_{12} for the FL and PL extracted from magnetometry measurements on reference films.

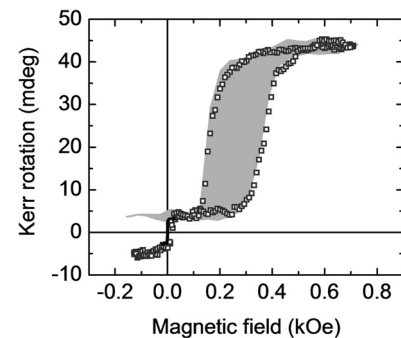| Stack	M_{FL}	M_{PL}	K_{FL}	K_{PL}	$H_{eb\,FL}$	$H_{eb\,PL}$	A_{12}
	(emu/cm^3)		($\times 10^3$ erg/cm^3)		(Oe)		($\times 10^{-3}$ erg/cm^2)
TV	930	1700	4.05	156	32.3	241	-7.48
PL ref.		1630		114		245	
FL ref.	930		5.12		0		

FIG. 1. Focused Kerr hysteresis loops corresponding to the component of magnetization parallel to a magnetic field applied along the easy axis and exchange bias axis of the FL and PL, respectively. Loops acquired from the center of each 6 μm disc are shown for the TV (dark grey open square symbols), and the PL (grey shaded loop) and FL (black line) reference discs.
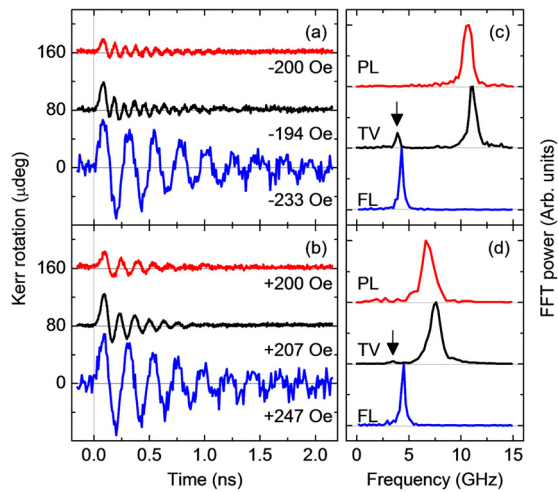
FIG. 2. TR Kerr signals acquired from the centre of each 6 μm disc are shown for the TV (black line), PL (red line), and FL (blue line) reference discs in (a) and (b) for parallel and anti-parallel FL states with respect to the PL following saturation in the direction of the exchange bias field. In (c) and (d), FFT spectra corresponding to TR signals in (a) and (b) are shown.

the TV. While the PL amplitude is approximately 3× to 4× smaller than that of the FL, the TV response is clearly dominated by the PL exhibiting the higher frequency precession observed in the PL reference disc. In Figure 2(a) beating of the TR signal is clearly observed for the TV. Fast Fourier transform (FFT) spectra calculated from the TR signals in Figures 2(a) and 2(b) are shown in Figures 2(c) and 2(d). As expected by inspection of the TR signals, comparison with the PL reference spectra reveal that the TV response is dominated by the PL. The FFT for the FL reference disc confirms that the lower frequency, smaller amplitude peak in the TV spectrum corresponds to the FL. In Figure 2(d), the frequency of the FL response (arrow) is similar when a magnetic field of the same magnitude, but opposite sign is applied. Because of the PL exchange bias and large anisotropy field, the PL remains parallel to the negative field

direction, but antiparallel to the FL, and exhibits a frequency that is lower than in the parallel case.

The full frequency dependence of the TV response on the applied magnetic field is shown for an increasing field sweep in Figure 3(a). The frequencies of the FL and PL reference discs are also overlaid. Since no exchange bias is present in the FL reference disc, TR measurements were only performed at field values in the range from the saturating magnetic field to zero for increasing and decreasing field sweeps. Both sweep directions are shown in Figure 3(a) since no difference in frequency is expected.[13] The minima in the frequency dependence in Figure 3(a) are well correlated with reversal peaks in the derivative of the TV hysteresis loop in Figure 3(c). For example, the jump in frequency from 5.9 to 10.4 GHz between 305 and 410 Oe coincides with the PL peak in Figure 3(c). Around the PL switching field, the frequency of the FL in the TV departs by ~1.2 GHz from that expected from the measurements on the FL reference disc. This implies dependence of the FL response on the magnetic state of the PL during switching.

In Figure 3(d), the dependence of frequency on the applied field is shown for the decreasing field sweep. In Figure 3(d), the FL frequency in the TV was very similar to that of the reference FL as the applied field was reduced to remanence. This suggests the magnetic state of the PL has little or no effect on the dynamics in the FL, particularly in the field range from 410 to 305 Oe in which it was observed to vary for increasing field sweep.

In Figures 3(b) and 3(e), the frequency linewidth of the FL and PL in the TV disc and of the FL reference disc are shown. The linewidth was extracted from Lorentzian fits of resonance peaks in the FFT spectra. In Figures 3(b) and 3(e), respectively, the reference FL linewidth is slightly lower than that in the TV disc. For both field sweeps the FL linewidth in the TV disc was observed to be enhanced around the FL and PL switching fields, particularly at the PL switching field.[14] It is clear that the presence of the PL in the TV has a marked effect on the linewidth and
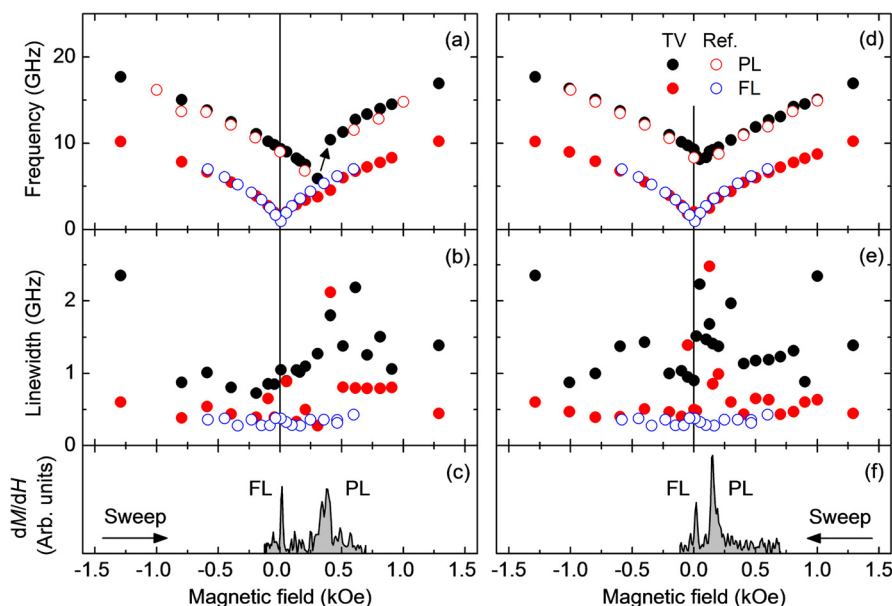

FIG. 3. The dependence of the precession frequency (a) and linewidth (b) on the applied magnetic field is shown for the tunnel valve stack (black and red filled symbols), and pinned (red open symbols) and free layer (blue open symbols) reference stacks for the increasing sweep after saturation parallel to the exchange bias direction. In (c), the derivative of the corresponding sweep of the Kerr hysteresis loop acquired from the tunnel valve 6 μm disc is shown. In (d), (e), and (f) the same data are shown for decreasing field sweep after anti-parallel saturation. In (b) and (e), the linewidth for the reference pinned layer is not shown.

relaxation rate of the FL as observed in the TR signals in Figures 2(a) and 2(b).

In the TV disc, Figures 3(b) and 3(e) generally show the PL to have a significantly larger linewidth than the FL. This is understood to be due to the strong exchange bias acting on the PL.[3,15] However, at the PL switching field, the linewidth of the FL and PL may become similar, for example, ∼2 GHz at 400 Oe in Figure 3(b). Macrospin model calculations (not shown) performed in the quasi-alignment limit and accounting for damping reveal that the FL and PL linewidths become similar around the PL switching field.

The similarity in the FL and PL linewidth can be understood in terms of the collective modes of the coupled FL-PL system. The linewidth is a collective property of the coupled system, where each contribution scales as the square of the precession amplitude.[16,17] In the TV disc, the precessional modes of the FL and PL both contribute to the linewidth. Far from the switching region, the frequencies of the two modes are very different and each mode has a clear character, since either the FL or PL provides the dominant contribution to the dynamics. Near the PL switching field, the frequency of the PL mode becomes similar to that of the FL (Figure 3(b) at ∼400 Oe). This allows the modes to mix and contribute to the collective linewidth, which may be further enhanced by inhomogeneous broadening associated with micromagnetic non-uniformities in the switching region.[14]

In summary, TR Kerr measurements have been performed on a microscale TV disc, and individual FL and PL reference discs. Focussed Kerr magnetometry was used to acquire hysteresis loops from the discs to understand the magnetic field dependence of the observed magnetization dynamics. The TR measurements revealed that the amplitude of the FL precession was significantly reduced in the TV stack, while the relaxation rate was enhanced. At the FL and PL switching fields, the FL linewidth was significantly enhanced. This was interpreted as a result of the formation of collective precessional modes of the FL and PL near to the switching field of the PL as its precession frequency approached that of the FL. Understanding of the influence of the coupling fields on the magnetisation dynamics in multi-layered magnetic structures is important for the development of nanoscale high frequency devices.

[1]I. N. Krivorotov, N. C. Emley, J. C. Sankey, S. I. Kiselev, D. C. Ralph, and R. A. Buhrman, Science **307**, 228 (2005).

[2]T. Gerrits, H. A. M. van den Berg, J. Hohlfeld, L. Bar, and T. Rasing, Nature **418**, 509 (2002).

[3]N. Smith, M. J. Carey, and J. R. Childress, Phys. Rev. B **81**, 184431 (2010).

[4]G. Woltersdorf, O. Mosendz, B. Heinrich, and C. H. Back, Phys. Rev. Lett. **99**, 246603 (2007).

[5]J. R. Childress, M. M. Schwickert, R. E. Fontana, M. K. Ho, P. M. Rice, and B. A. Gurney, J. Appl. Phys. **89**, 7353 (2001).

[6]P. S. Keatley, V. V. Kruglyak, A. Neudert, E. A. Galaktionov, R. J. Hicken, J. R. Childress, and J. A. Katine, Phys. Rev. B **78**, 214412 (2008).

[7]J. H. H. Rietjens, C. Józsa, W. J. M. de Jonge, B. Koopmans, and H. Boeve, Appl. Phys. Lett. **87**, 172508 (2005).

[8]J. H. H. Rietjens, C. Jozsa, H. Boeve, W. J. M. de Jonge, and B. Koopmans, J. Magn. Magn. Mater. **290–291**, 494 (2005).

[9]P. S. Keatley, V. V. Kruglyak, R. J. Hicken, J. R. Childress, and J. A. Katine, J. Magn. Magn. Mater. **306**, 298 (2006).

[10]B. D. Schrag, A. Anguelouch, G. Xiao, P. Trouilloud, Y. Lu, W. J. Gallagher, and S. S. P. Parkin, J. Appl. Phys. **87**, 4682 (2000).

[11]V. V. Kruglyak, A. Barman, R. J. Hicken, J. R. Childress, and J. A. Katine, Phys. Rev. B **71**, 220409(R) (2005).

[12]Cavity enhancement of the Kerr rotation using a ZnS (33 nm) layer was used on the TV stack. The Kerr rotation has been scaled appropriately for comparison with the uncapped FL and PL reference discs.

[13]The same FL data are shown in Figures 3(a) and 3(b) since the FL frequency dependance is not expected to depend on the magnetic field sweep direction when the applied field is larger than the anisotropy field.

[14]J. F. Sierra, F. G. Aliev, R. Heindl, S. E. Russek, and W. H. Rippard, Appl. Phys. Lett. **94**, 012506 (2009).

[15]X. Joyeux, T. Devolder, J.-V. Kim, Y. Gomez de la Torre, S. Eimer, and C. Chappert, J. Appl. Phys. **110**, 063915 (2011).

[16]A. M. Zyuzin, A. G. Bazhanov, S. N. Sabaev, and S. S. Kidyaev, Phys. Solid State **42**, 1317 (2000).

[17]V. V. Kruglyak and A. N. Kuchko, Phys. Met. Metall. **92**, 211 (2001).